Journal of Materials Science: Materials in Electronics
https://doi.org/10.1007/s10854-019-01208-0

REVIEW

Investigation on phase and microstructures of a temperature stable high-Q $Li_2Zn_{0.95}Sr_{0.05}Ti_3O_8$ microwave dielectric ceramic

Haishen Ren[1] · Zhilun Wu[1,2] · Fei He[1] · Yi Zhang[1] · Xiangyu Zhao[1] · Xiaogang Yao[1] · Huixing Lin[1]

Received: 31 January 2019 / Accepted: 22 March 2019

Abstract
A temperature stable high-Q $Li_2Zn_{0.95}Sr_{0.05}Ti_3O_8$ microwave dielectric ceramic is fabricated by conventional solid-state reaction route and the phase composition, microstructures and microwave dielectric properties are investigated in this paper. The bulk density and FESEM results indicate that this ceramic can be well-sintered at 1075 °C for 4 h. Since the difficulty in Sr^{2+} ions diffused into the $Li_2ZnTi_3O_8$ crystal lattice to form solid solutions owing to the large radii difference between Sr^{2+} (1.44Å) and Zn^{2+} (0.74Å), there are three phases including the main phase $Li_2ZnTi_3O_8$ and the second phase $SrTiO_3$ and unknown phase according to the XRD and element-distribution mapping results. The formation of second phase is advantageous to improve the relative permittivity (ε_r) and temperature coefficient of resonant frequency (τ_f), but degrades the quality factor (Q × f) slightly. The $Li_2Zn_{0.95}Sr_{0.05}Ti_3O_8$ ceramic sintered at 1075 °C/4 h displays a temperature stable high-Q properties: $\varepsilon_r = 26.6$, Q × f = 62300 GHz, and $\tau_f = 0.27$ ppm/°C.

1 Introduction

In the era of information explosion, high performance microwave dielectric ceramics as the basic materials of filter, antenna and resonator components play a more and more important role in new-style telecommunication technology such as fifth generation wireless systems, internet of things, the industrial internet, satellite broadcasting, intelligent transport systems and so on [1, 2]. There are three properties simultaneously satisfied for ideal microwave dielectric ceramic materials from the device design point of view: appropriate relative permittivity (ε_r, low-ε_r for millimeter-wave communication and substrate materials, medium-ε_r for satellite communications and cellphone base stations, and high-ε_r for miniaturization of mobile terminal equipment), high quality factor (Q × f ≥ 50,000 GHz, for the good frequency selectivity of device), near zero temperature coefficient of resonant frequency ($\tau_f \leq \pm 10$ ppm/°C, for the stability of the frequency against temperature change) [2, 3]. Unfortunately, most of these ceramic materials with appropriate relative permittivity and high quality factor cannot be used for commercial application due to excessive positive or negative zero temperature coefficient of resonant frequency. Therefore, it is both a key and a difficult point to adjust the τ_f to near zero and maintain high Q × f value as much as possible synchronously.

Nowadays, there are two dominant methods applied for producing a material with near zero temperature coefficient of resonant frequency [4, 5]: (a) Composite materials by mixing component materials with negative and positive τ_f values, such as $Mg_4Ta_2O_9$ (−70 ppm/°C)–$MgTa_2O_6$ (+56 ppm/°C) [6], $Li_2Zn_3Ti_4O_{12}$ (−48 ppm/°C)–TiO_2 (+456 ppm/°C) [5], $Mg_6Ti_5O_{16}$ (−50 ppm/°C)–$Ca_{0.8}Sr_{0.2}TiO_3$ (+991 ppm/°C) [7]. (b) Solid solutions ceramic materials through adjustment structure, for instance $A(B'_{1/3}B''_{2/3})O_3$ (A = Sr, Ba, B′ = Zn, Mg, B″ = Ta, Nb) complex perovskite system and (Zr,Sn)TiO_4 system [8–10]. Recently, $Li_2ZnTi_3O_8$ ceramic has been extensively investigated because of low sintering temperature (1075 °C for 4 h) and good microwave dielectric properties ($\varepsilon_r = 25.6$, Q × f = 72,000 GHz and $\tau_f = -11.2$ ppm/°C) [11]. These advantages make it as a promising material for the applications in dielectric antennas and dielectric resonators except for excessive negative τ_f value which impedes its application. In fact, some work has been done to modify the

✉ Haishen Ren
renhaishen@mail.sic.ac.cn

✉ Huixing Lin
huixinglin@mail.sic.ac.cn

[1] Key Laboratory of Inorganic Functional Material and Device, Shanghai Institute of Ceramics, Chinese Academy of Sciences, Shanghai 200050, China

[2] Department of Materials, Chongqing University of Technology, Chongqing 400050, China

Published online: 28 March 2019

τ_f value to near-zero by adding large positive τ_f (e.g. TiO_2, $CaTiO_3$ +859 ppm/°C) [5, 12]. For instance, Bari et al. [4] reported that the TiO_2 nanoparticles additive on $Li_2ZnTi_3O_8$ ceramic not only obtained optimal dielectric properties ($\varepsilon_r = 28$, $Q \times f = 68{,}000$ GHz, and $\tau_f = -2$ ppm/°C), but also the sintering temperature was reduced to 1050 °C. George and Sebastian [12] found that when Ca ion substitutes for Zn ion of $Li_2ZnTi_3O_8$, the second phase $CaTiO_3$ phase form in $Li_2(Zn_{1-x}Ca_x)Ti_3O_8$ ($0 \le x \le 0.2$) system, which can make the τ_f value of $Li_2ZnTi_3O_8$ to near zero due to the large positive τ_f of $CaTiO_3$ phase. Typically, the $Li_2Zn_{0.095}Ca_{0.05}Ti_3O_8$ ceramics displayed excellent comprehensive properties of $\varepsilon_r = 27$, $Q \times f = 40{,}000$ GHz and $\tau_f = -2$ ppm/°C. Hence, it is effective method for adjusting the τ_f of $Li_2ZnTi_3O_8$ ceramic to near-zero by mixing with the positive τ_f value of ceramic materials. Besides, $SrTiO_3$ ceramic has bigger positive τ_f value than $CaTiO_3$. In present paper, the sintering behaviors, phases, microstructures and microwave dielectric properties of $Li_2Zn_{0.95}Sr_{0.05}Ti_3O_8$ ceramic will be investigated in detail.

2 Experimental

The $Li_2Zn_{0.95}Sr_{0.05}Ti_3O_8$ powders were synthesized by the conventional solid-state-reaction method using stoichiometry of high-purity raw materials (99.9%, Sinopharm Chemical Reagent Co. Ltd, China), namely Li_2CO_3, ZnO, $SrCO_3$ and TiO_2. The mixture mixed in a Nylon tank using ethyl alcohol and ZrO_2 balls as media by planetary ball mill for 2 h were dried at 110 °C for 4 h and then calcined at 900 °C for 8 h. Subsequently, the calcined powders were planetary-milled with ZrO_2 balls and ethyl alcohol for 2 h. After drying, the obtained powder were granulated by adding 8 wt.% polyvinyl alcohol solution and screened through a 40-mesh sieve for getting the uniformity particle size and good fluidity power. Preformed pellets of 15 mm in diameter and 8 mm in height were obtained from the powder using a cylindrical steel mold, and then were pressed at 2 MPa by hydraulic pressing, followed by sintering between 1000 °C and 1125 °C for 4 h in air at a heating rate of 5 °C/min.

The phase compositions present in sintered samples were identified by X-ray diffraction analysis with a Cu/Kα radiation (XRD, D8 ADVANCE, Bruker, Germany). The microstructure characteristics of the sintered samples was observed by field emission scanning electron microscope (FESEM, Magellan 400, FEI Company, USA) equipped with an energy dispersive spectroscopy (EDS). The bulk density of sintered samples was measured applying the Archimedes' method. The dielectric constant and dielectric loss (tanδ) of the samples with the diameter of 12 mm and the height of 6 mm were collected by the Hakki–Coleman dielectric resonator method in the TE011 mode using an Agilent E8363A PNA series network analyzer. The Q value were calculated from the value in the light of the $Q = 1/\tan\delta$. The τ_f value was measured over the range from 25 to 85 °C heating through the temperature test cabinet (VTL7003, Vötsch, Germany), and was calculated by following equation:

$$\tau_f = \frac{f_{85} - f_{25}}{60 \times f_{25}} \times 10^6 (\text{ppm/°C})$$

where f_{85} and f_{25} represent the resonant frequencies at 85 °C and 25 °C, respectively.

3 Results and discussion

Figure 1 shows the X-ray diffraction patterns of $Li_2ZnTi_3O_8$ and $Li_2Zn_{0.95}Sr_{0.05}Ti_3O_8$ ceramics sintered at 1075 °C for 4 h. It can be found from Fig. 1a that the pure phase of the cubic spinel structure $Li_2ZnTi_3O_8$ (JCPDS no. 44-1037, P4332 (212)) ceramic is formed and there are no additional diffraction peaks to indicate secondary phase existed, such that the as-sintered sample is single-phase pure. However, the weak diffraction peaks of secondary phase corresponding to cubic structure $SrTiO_3$ (JCPDS no. 35-0734, Pm-3m (211)) and unknown phase appeared in the XRD patterns shown in Fig. 1b of $Li_2Zn_{0.95}Sr_{0.05}Ti_3O_8$ as-sintered samples except for the high peaks of $Li_2ZnTi_3O_8$ phase. The appearance of the second phase might be ascribed to the fact that the difficulty in Sr ions diffuses into the $Li_2ZnTi_3O_8$

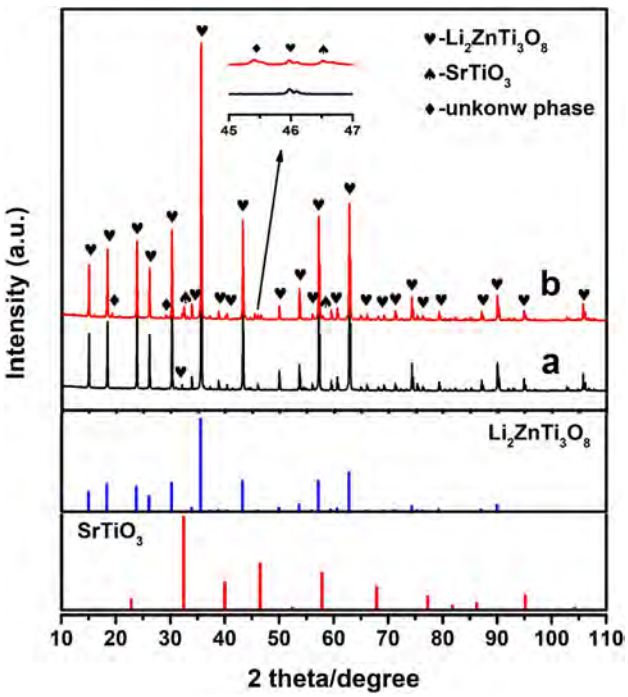

Fig. 1 XRD patterns of $Li_2ZnTi_3O_8$ (***a***) and $Li_2Zn_{0.95}Sr_{0.05}Ti_3O_8$ (***b***) ceramics sintered at 1075 °C for 4 h

crystal lattices and forms solid solutions due to relatively large Sr ions (1.44Å) compared to Zn ions (0.74Å) [1]. This results is consistent with the Fang, George and Zhao [12–14] reports that when Ca ions instituted for Zn or Mg ions in Li_2O–AO–TiO_2 (A = Zn, Mg) system, the secondary phase $CaTiO_3$ was obtained in this system that is advantageous to adjusting the dielectric properties, near-zero τ_f value in particular, and reducing the Li evaporation during sintered process. Hence, the formation of $SrTiO_3$ phase in our work will help τ_f value of $Li_2ZnTi_3O_8$ shift to near zero by mixing component materials with negative and positive τ_f values.

Figure 2 displays the SEM microstructures of natural surface of $Li_2Zn_{0.95}Sr_{0.05}Ti_3O_8$ ceramics sintered at various temperatures from 1000 to 1075 °C for 4 h. As Fig. 2a shown, a porous microstructure with fine particle size (less than 10um, inset) can be seen for sample sintered at 1000 °C. With the sintered temperature increasing to 1050 °C, the densification of specimen gradually increases that there are few pores around the grain boundaries and yet some pores distributed on the big grains presented in Fig. 4b–c. Beyond that, it is found that two sizes of grain, large one more than 100um (see arrow) and small one (circle) still about 10um, in these microstructures. To identify the chemical composition of two grains, the element-distribution mapping (EDM) and energy dispersive X-ray analysis (EDX) is carried out on natural surface of ceramic sintered at 1075 °C for 4 h shown in Figs. 3 and 4. It can be seen from Fig. 3 that large grains has a composition rich in O, Zn and Ti element and meanwhile the EDX analysis of Spot C explains that they mainly contain O, Zn and Ti elements in an approximate molar ratio of O:Zn:Ti = 8:3:1, indicating that these grains is $Li_2ZnTi_3O_8$ phase. The small grains are richer in O, Sr and Ti element, but the EDX data of small grains (marked A and B) reveal that these is minute quantities of Zn elements expect for primary O, Ti and Sr. It means that ZnO ion maybe react with SrO and TiO_2 phase leading to form unknown phase during sintering process, and small grains include $SrTiO_3$ phase and unknown phases. This results also illustrate that with increasing of sintering temperature the $Li_2ZnTi_3O_8$ grains gradually grow up and yet $SrTiO_3$ phase grains remain the same due to higher densification temperature (1300–1400 °C) of $SrTiO_3$ ceramic. Sintering temperature further to 1075 °C, the amount of the pore on $Li_2ZnTi_3O_8$ grains decreases and the sizes of $SrTiO_3$ grains increases somewhat.

Figure 5 summaries the bulk density (a), relative permittivity (b) and Q × f value (c) of $Li_2Zn_{0.95}Sr_{0.05}Ti_3O_8$ ceramic as a function of temperature for 4 h. It is noticed from Fig. 5a that the bulk density of sintered samples increases from 3.45 to 3.98 g/cm^3 with increasing the sintering temperatures from 1000 to 1075 °C, and then slightly declines after 1075 °C, implying the substitution Sr for Zn has no impact on the densification process of ceramic. The variation of the relative permittivity and Q × f value in regard to temperature has a similar tendency with bulk density as shown in Fig. 5b, c. For microwave dielectric composite ceramics, relative permittivity is dictated to sintering densification, the phase composition and its relative contents [15]. Obviously, the relative permittivity raises from 25.8 to 26.6 with the increasing sintering temperature from 1000 to 1075 °C due to the densification process. It is noteworthy that the permittivity of $Li_2Zn_{0.95}Sr_{0.05}Ti_3O_8$ ceramic is higher that of

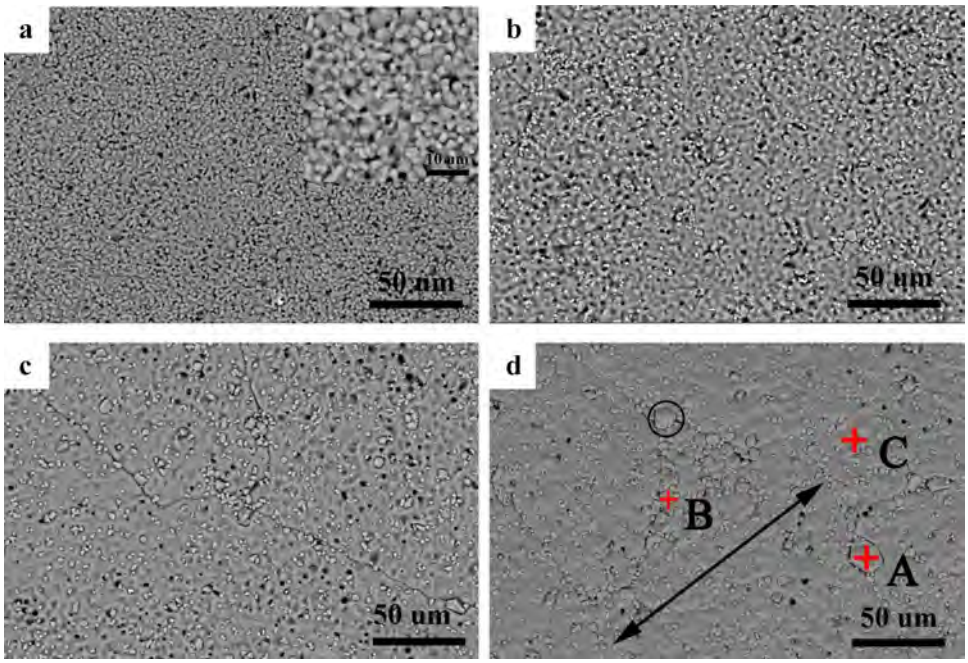

Fig. 2 The SEM microstructures of the surface of $Li_2Zn_{0.95}Sr_{0.05}Ti_3O_8$ ceramics sintered at various temperature: **a** 1000, **b** 1025, **c** 1050, **d** 1075 °C for 4 h

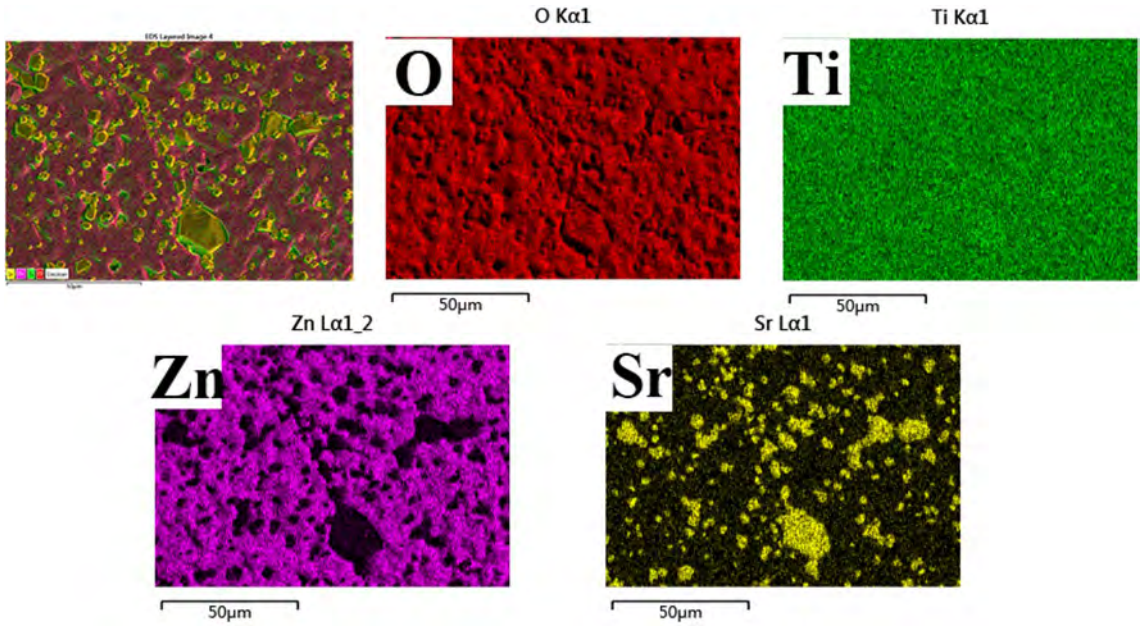

Fig. 3 The element-distribution mapping of $Li_2Zn_{0.95}Sr_{0.05}Ti_3O_8$ ceramics sintered at 1075 °C for 4 h

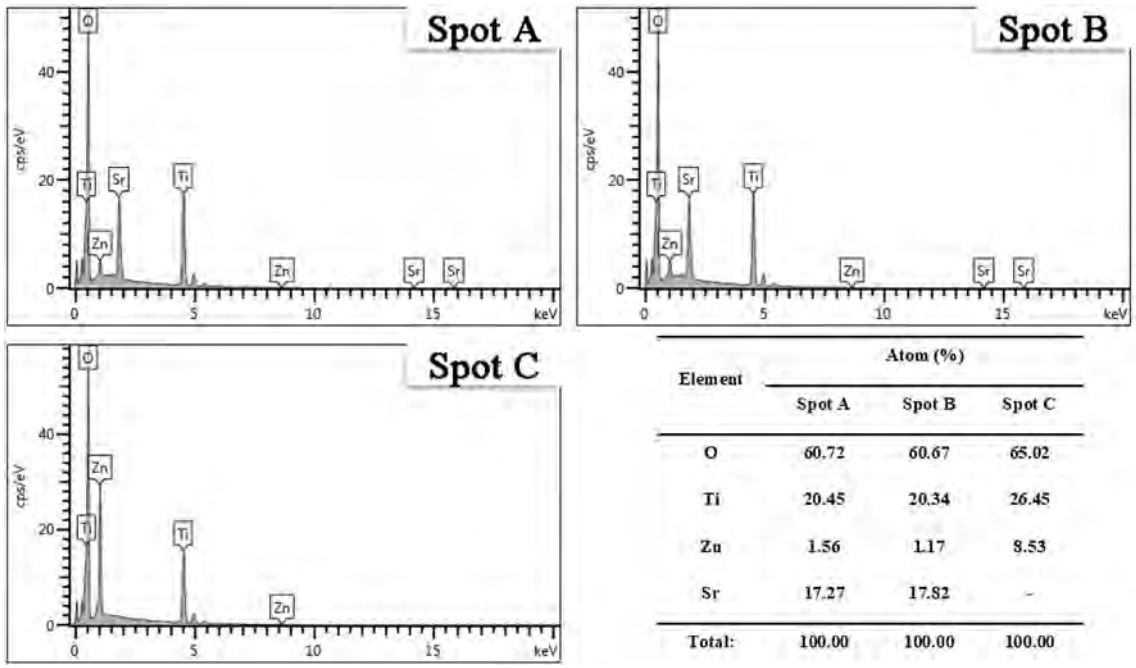

Element	Atom (%)		
	Spot A	Spot B	Spot C
O	60.72	60.67	65.02
Ti	20.45	20.34	26.45
Zn	1.56	1.17	8.53
Sr	17.27	17.82	-
Total:	100.00	100.00	100.00

Fig. 4 The energy dispersive X-ray analysis and data on the marked areas of $Li_2Zn_{0.95}Sr_{0.05}Ti_3O_8$ ceramics sintered at 1075 °C for 4 h

pure $Li_2ZnTi_3O_8$ ceramic (25.6), and this could be the reason for the appearance formation of high-ε_r $SrTiO_3$ phase. The microwave dielectric loss for composite ceramics is mainly caused by the porosity, second phases, grain sizes, etc. [16]. In this case, the porosity and second phases mainly dominate the dielectric loss. The highest Q × f value (63,000 GHz) are obtained at 1075 °C when maximum sintering density are observed. All in all, the promising microwave dielectric properties of $\varepsilon_r = 26.6$, Q × f = 62,300 GHz, and $\tau_f = 0.3$ ppm/°C can be obtained at 1075 °C for 4 h. Table 1 exhibits comparison of the microwave dielectric properties of recently reported $Li_2ZnTi_3O_8$ ceramic materials, which

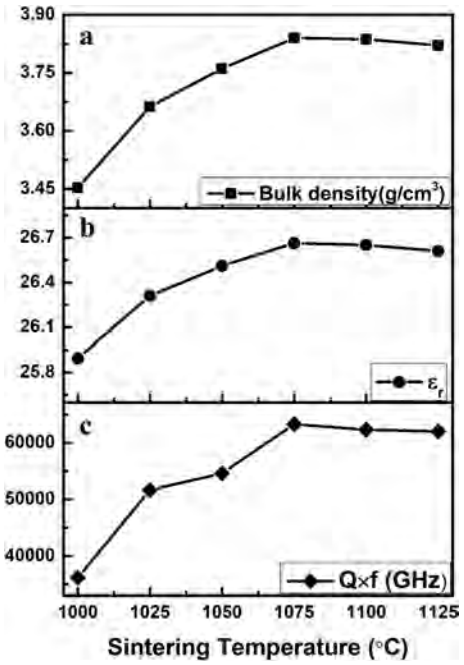

Fig. 5 The bulk density (**a**), relative permittivity (**b**) and Q×f value (**c**) of $Li_2Zn_{0.95}Sr_{0.05}Ti_3O_8$ ceramic as a function of temperature for 4 h

demonstrates that the $Li_2Zn_{0.95}Sr_{0.05}Ti_3O_8$ ceramic material in our work displays excellent comprehensive microwave dielectric properties with high Q×f value and near zero τ_f value synchronous.

4 Conclusions

In the paper, the temperature stable high-Q $Li_2Zn_{0.95}Sr_{0.05}Ti_3O_8$ ceramic material has been synthesized and investigated. The results show that there are three phases including main phase $Li_2ZnTi_3O_8$ and second phase $SrTiO_3$ and unknown phase in this ceramic sintered at 1075 °C for 4 h. With the increase of sintering temperature from 1000 to 1125 °C, the bulk density, ε_r and Q×f value of $Li_2Zn_{0.95}Sr_{0.05}Ti_3O_8$ ceramic firstly increase and then decrease. The highest ε_r (26.6) and Q×f value (62,300 GHz) are obtained at 1075 °C when maximum sintering density (3.98 g/cm^3) are observed, which $Li_2Zn_{0.95}Sr_{0.05}Ti_3O_8$ ceramic has optimal comprehensive microwave dielectric properties with high Q×f value and near zero τ_f value (0.3 ppm/ °C) synchronous.

Table 1 The microwave dielectric properties and sintering temperature of recently reported $Li_2ZnTi_3O_8$ ceramic materials

Composition	ε_r	Q×f (GHz)	τ_f (ppm/°C)	T_s (°C)	Second phase	Refs.
$Li_2ZnTi_3O_8$	25.6	72,000	−11.2	1075 °C/4 h	–	[11]
4 wt% nano-TiO_2 + $Li_2ZnTi_3O_8$	28	68,000	−2	1050 °C/4 h	TiO_2	[4]
Pretreating raw materials $Li_2ZnTi_3O_8$	25.8	74,200	−13	950 °C/4 h	–	[17]
Reaction sintering process $Li_2ZnTi_3O_8$	23.3	77,100	−12.4	1025 °C/4 h	–	[18]
Annealing treatment $Li_2ZnTi_3O_8$	25.6	90,000	−10.8	1075 °C/4 h	–	[19]
Controlled heating rates $Li_2ZnTi_3O_8$	26.6	83,000	−12.4	1075 °C/4 h		[20]
$Li_2Zn_{1.06}Ti_3O_8$	25.5	63,000	−18	1075 °C/4 h	–	[21]
$Li_2Zn(Ti_{0.93}Zr_{0.07})_3O_8$	25.4	122,000	−16	1100 °C/4 h	ZrO_2	[22]
$Li_2ZnTi_3O_8$-0.2 mol SnO_2	20.9	89,500	−24	1080 °C/4 h	SnO_2	[23]
$Li_2Zn_{0.94}Mg_{0.06}Ti_3O_8$	26.1	150,000	−13.9	1140 °C/2 h	–	[24]
$Li_2Zn_{0.92}Co_{0.08}Ti_3O_8$	24.7	140,000	−13.4	1140 °C/2 h	–	
$Li_2Zn_{0.94}Co_{0.06}Ti_3O_8$	26.2	90,400	−11.4	1075 °C/4 h	–	[25]
$Li_2ZnTi_3O_{8-x}Al_2O_3$ (x = 0–8 wt.%)	26.2 ~ 17.9	66,000 ~ 30,000	−11.6 ~ −17.9	1075~1150 °C/4 h	TiO_2 $ZnAlO_3$	[26]
$Li_2Zn_{0.95}Ca_{0.05}Ti_3O_8$	27	52,000	−3	1075 °C/4 h	$CaTiO_3$	[12]
$Li_2ZnTi_{3.04}O_{8.12}$	25.8	63,400	−8.1	1100 °C/4 h	TiO_2	[27]
$Li_2ZnTi_{3.06}O_{8.18}$	25.9	47,500	−3.2	1100 °C/4 h	TiO_2	
$Li_2Zn_{0.95}Sr_{0.05}Ti_3O_8$	26.6	62,300	0.3	1075 °C/4 h	$SrTiO_3$	This paper

Ts sintering temperature, *Refs* references

References

1. M.T. Sebastian, *Dielectric Materials for Wireless Communication*, 1st edn. (Elsevier, Oxford, 2008)
2. H. Ohsato, J. Ceram. Soc. Jpn. **113**, 703–711 (2005)
3. M.T. Sebastian, R. Ubic, H. Jantunen, Int. Mater. Rev. **60**, 392–412 (2015)
4. M. Bari, E. Taheri-Nassaj, H. Taghipour-Armaki, J. Am. Ceram. Soc. **96**, 3737–3741 (2013)
5. X.B. Liu, H.F. Zhou, X.L. Chen, L. Fang, J. Alloys Compd. **515**, 22–25 (2012)
6. M.Z. Dang, H.S. Ren, X.G. Yao, H.Y. Peng, T.Y. Xie, H.X. Lin, L. Luo, J. Am. Ceram. Soc. **101**, 3026–3031 (2018)
7. J. Zhang, Y. Luo, Z.X. Yue, L.T. Li, Ceram. Int. **44**, 141–145 (2018)
8. S. Nomura, K. Toyama, K. Kaneta, Jpn. J. Appl. Phys. 2 **21**, L624–L626 (1982)
9. W.C. Tzou, Y.C. Chen, C.F. Yang, Mater. Res. Bull. **41**, 1357–1363 (2006)
10. D. Pamu, G.L.N. Rao, K.C. James Raju, J. Am. Ceram. Soc. **95**, 126–132 (2012)
11. S. George, M.T. Sebastian, J. Am. Ceram. Soc. **93**, 2164–2166 (2010)
12. S. George, M.T. Sebastian, J. Eur. Ceram. Soc. **30**, 2585–2592 (2010)
13. Z.X. Fang, B. Tang, F. Si, S.R. Zhang, Ceram. Int. **43**, 1682–1687 (2017)
14. X.G. Zhao, Bull. Chin. Ceram. Soc. **33**, 401–404 (2014)
15. H.S. Ren, M.Z. Dang, H.J. Wang, T.Y. Xie, S.H. Jiang, H.X. Lin, L. Luo, Mater. Let. **210**, 113–116 (2018)
16. J.B. Song, K.X. Song, J.S. Wei, H.X. Lin, J.M. Xu, J. Wu, W.T. Su, J. Alloys Compd. **731**, 264–270 (2018)
17. H.F. Zhou, N. Wang, X.H. Tan, J. Huang, X.L. Chen, J. Mater. Sci. Mater. Electron. **27**, 11850–11855 (2016)
18. X.P. Lu, Y. Zheng, Z.W. Dong, W.Y. Zhang, Q. Huang, J. Mater. Sci. Mater. Electron. **25**, 3358–3363 (2014)
19. T.A. Hamid, T.N. Ehsan, M. Bari, J. Alloys Compd. **581**, 757–761 (2013)
20. X.P. Lu, Y. Zheng, Q. Huang, W.H. Xiong, J. Electron. Mater. **44**, 4243–4249 (2015)
21. M. Parastoo, T.N. Ehsan, T.A. Hamid, J. Alloys Compd. **695**, 3772–3778 (2017)
22. J. Zhang, R.Z. Zuo, J. Mater. Sci. Mater. Electron. **26**, 9219–9224 (2015)
23. P. Zhang, Y.G. Zhao, Ceram. Int. **42**, 2882–2886 (2016)
24. C.L. Huang, C.H. Su, C.M. Chang, J. Am. Ceram. Soc. **94**, 4146–4149 (2011)
25. X.P. Lu, Z.W. Dong, Y. Zheng, J. Electron. Mater. **46**, 6977–6983 (2017)
26. J.Q. Ren, K. Bi, X.L. Fu, Z.J. Peng, Ceram. Int. **44**, 8928–8933 (2018)
27. Y. Sadin, E.T. Nassaj, H.T. Armaki, W.Z. Lu, W. Lei, H.B. Bafrooei, J. Mater. Sci. Mater. Electron. **29**, 13516–13525 (2018)